

ECE APPLIED TO ENERGY FROM SPACE-TIME:
AMPLIFICATION OF THE RADIATIVE CORRECTION BY
SPIN CONNECTION RESONANCE.

by

Myron W. Evans,

Civil List Scientist,

and

H. Eckardt and G. J. Evans,

A.I.A.S.

(Contact: emyrone@aol.com, www.aias.us)

ABSTRACT

The well known radiative correction is amplified by spin connection resonance, whereby the initially Coulombic potential in an easily ionized material is amplified to the point where electrons are released for use in circuits, energy production and energy savings. It is assumed that the radiative correction can be represented by an oscillating part of the fine structure constant. The methods of Einstein Cartan Evans (ECE) field theory are used to amplify the induced jitterbugging of the electron in each orbital that is the primary characteristic of the radiative correction. The latter is observed in well known phenomena such as the electron g factor, the Lamb shift and the Casimir effect. It is shown that the initially small radiative correction can be amplified for practical implementation.

Keywords: Einstein Cartan Evans (ECE) field theory, radiative correction, spin connection resonance amplification, new sources of energy.

Paper 87 of ECE Series

Recently the Einstein Cartan Evans (ECE) field theory has offered a generally covariant unified field theory based on the principles of relativity - that physics is objective and causal {1-11}. Relativity is the most precise theory of physics. Electrodynamics and quantum mechanics have been forged together with gravitation and the other fundamental force fields in one theoretical framework based on Cartan geometry {12}. With these developments came the realization that the spin connection of space-time plays a central role in electrodynamics, which in ECE is considered to be a theory of general relativity, not of special relativity. It has been shown {11} that the spin connection can produce amplification of gravitational effects, an amplification which may be used in counter-gravitational devices. In the field of electrodynamics it has been shown {1-11} that the spin connection may be used to amplify the repulsion between electrons in an atom or molecule to the point at which the electrons are freed from the nucleus and may be used in circuits to produce power or save power. Recently, it has been shown {1-11} that the Lamb shift may be explained within experimental precision by using an average effect of the ubiquitous zero'th eigenstate of the quantized electromagnetic field ("zero point energy") to describe the well known {13,14} radiative correction. The Lamb shift has been described in ECE theory in a manner that is consistent with the description of the g factor of the electron in earlier work {1-11}.

In Section 2 the radiative correction in the hydrogen atom is considered to arise from an oscillating component of the averaged radiative correction used in previous work {1-11}. The Lamb shift is illustrated in atomic hydrogen for this type of radiative correction. The charge density in each orbital is calculated for each orbital. In Section 3 these charge densities are used in the generally covariant Coulomb law of ECE theory and it is shown that the radiative correction in each orbital of atomic hydrogen can be amplified by spin connection resonance to the point at which the electron breaks free ~~from~~^{so} the proton and may be used in a

circuit to produce power. This process is known as “energy from space-time”. This paper therefore identifies the driving term of the spin connection resonance mechanism as the radiative correction. The latter causes zitterbewegung, the well known {15} jitterbugging of the electron in each orbital due to the ubiquitous, background, radiative correction. The latter is due to the fact that in the quantized electromagnetic field surrounding the atom, there are ever present and ever oscillating electric and magnetic fields. In the zero'th eigenstate of the quantized, background, electromagnetic field these electric and magnetic fluctuations exist when there are no photons {15} present, the photon being defined as the quantum of energy. The electromagnetic potential due to these fluctuating electric and magnetic fields produces well known phenomena such as the g factor of the electron and other particles, the Lamb shift, and the Casimir effect. These are examples of the ways in which the radiative correction is observed experimentally. No energy is required to manufacture the potential of the radiative correction, which is therefore like an enormous natural reservoir of energy, one which is ever present. The natural effect of the radiative correction is very small (about four parts in ten million ^{for} atomic hydrogen), but in ECE theory (generally covariant unified field theory) it may be amplified by spin connection resonance {1-11}. In Section 4 the results of Sections 2 and 3 are developed numerically, and in Section 5 a discussion is given of the type of material most likely to release electrons through the theory of this paper. The hydrogen atom is used as a model for future work based on density functional code in solids.

2. RADIATIVE CORRECTION IN THE HYDROGEN ATOM.

In previous work on the electron g factor and Lamb shift {1-11} the mean value of the radiative correction was implemented as follows:

$$g \rightarrow g \left(1 + \frac{\langle \alpha \rangle}{4\pi} \right)^2 \quad - (1)$$

$$\nabla^2 \rightarrow \nabla^2 \left(1 + \frac{\langle d \rangle}{4\pi} \right)^2 - (2)$$

where g is the electron g factor, and where d is the fine structure constant. Eq. (1) was used with the Dirac equation derived from the ECE wave equation, and Eq. (2) was used with the Schrödinger equation. In order to model the jitterbugging of the electron it is assumed that:

$$d = \langle d \rangle \left(1 + \cos(\kappa r) \right) - (3)$$

where κ is a characteristic wave-number of the jitterbugging and where r is the radial coordinate {1-11}. The jitterbugging is therefore the initially small driving term of the spin connection resonance (SCR) mechanism of previous work {1-11}. The hydrogen atom is used to model the effect of Eq. (3) on each orbital.

To first order in d :

$$\left(1 + \frac{d}{4\pi} \right)^2 \sim 1 + \frac{d}{2\pi} = 1 + \frac{\langle d \rangle}{2\pi} \left(1 + \cos(\kappa r) \right) - (4)$$

and the Schrödinger equation of atomic hydrogen becomes:

$$-\frac{\hbar^2}{2m} \left(1 + \frac{\langle d \rangle}{2\pi} \left(1 + \cos(\kappa r) \right) \right) \nabla^2 \psi + V^{(0)} \psi = E \psi - (5)$$

where

$$V^{(0)} = -\frac{e^2}{4\pi \epsilon_0 r} - (6)$$

is the initially Coulombic attraction between the proton and electron. The effect of SCR is to amplify this attraction into a strong repulsion which allows the electron to break free from the proton. In Eq. (5), ψ is the wave-function and E is the total energy {15}. In Eq. (6), e

is the charge on the proton (minus the charge on the electron), and ϵ_0 is the vacuum permittivity in S.I. units {15}.

It is well known {15} that Eq. (5) can be developed into:

$$-\frac{\hbar^2}{2m} \left(1 + \frac{\alpha}{2\pi} \right) \frac{d^2 P}{dr^2} + \nabla_{\text{eff}}^{(0)} P = E P \quad - (7)$$

where:

$$P(r) = r R(r). \quad - (8)$$

Here R is the radial wave-function of the hydrogen atom. The potential energy in Eq. (7) is

$$\nabla_{\text{eff}}^{(0)} = -\frac{e^2}{4\pi\epsilon_0 r} + \frac{l(l+1)\hbar^2}{2mr^2} \quad - (9)$$

where l is the angular momentum quantum number, m is the mass of the electron and \hbar is the reduced Planck constant. The positive term in Eq. (9) is the well known centrifugal repulsion term in atomic hydrogen {15}. Using previous work {1-11} on the Lamb shift in atomic hydrogen and helium, Eq. (7) is re-written as:

$$-\frac{\hbar^2}{2m} \frac{d^2 P}{dr^2} + \nabla_{\text{eff}} P = E P \quad - (10)$$

where:

$$\nabla_{\text{eff}} = -\frac{e^2}{4\pi\epsilon_0 (r+r(\text{vac}))} + \frac{l(l+1)\hbar^2}{2m (r+r(\text{vac}))^2} \quad - (11)$$

Here r(vac) is a radial adjustment due to the radiative correction. It is different for each orbital and can be calculated by subtracting Eq. (10) from Eq. (7), giving:

$$-\frac{\hbar^2}{4\pi m} \frac{d}{dr} \frac{d^2 P}{dr^2} + \left(\nabla_{\text{eff}}^{(0)} - \nabla_{\text{eff}} \right) P = 0. \quad (12)$$

The known hydrogenic P may be used in Eq. (12) to compute r(vac) using computer algebra. This assumption is based on the experimental fact that the Lamb shift for atomic H splits the 2s and 2p levels by about four parts in ten million, so the hydrogenic wavefunctions are only slightly affected. In previous work the experimentally measured Lamb shift was explained in terms of an average r(vac) for the hydrogen and helium atoms. More accurately, as in this paper, r(vac) oscillates from Eq. (3), i.e. the electron jitterbugs in each orbital. The jitterbugging is the phenomenon used to build up the driving term of the SCR mechanism.

To construct the driving term, the charge density ρ in each orbital must be calculated, the driving term is then $-\rho/\epsilon_0$. In order to calculate ρ , it is necessary to calculate the probability of finding the electron in a volume element $d\tau$ at some point (r, θ, ϕ) in spherical polar coordinates {15}. This probability is:

$$d\rho_e = |\psi(r, \theta, \phi)|^2 d\tau. \quad (13)$$

The volume element is:

$$d\tau = r^2 dr \sin \theta d\theta d\phi. \quad (14)$$

The probability of finding the electron in a spherical shell of thickness dr and radius r is the sum over these probabilities {15} as θ and ϕ move over the range:

$$0 \leq \theta \leq \pi, \quad 0 \leq \phi \leq 2\pi. \quad (15)$$

This sum is:

$$P_e = \int_0^\pi \sin \theta d\theta \int_0^{2\pi} |\psi(r, \theta, \phi)|^2 d\phi dr. \quad - (16)$$

However, the P function of Eq. (7) depends only on r, so the summed probability is:

$$P_e = 4\pi r^2 P. \quad - (17)$$

If we consider the probability to be determined by R itself, rather than P, then the summed probability is:

$$P_e = 4\pi r^2 R. \quad - (18)$$

The use of Eq. (17) or (18) is a matter of choice. If we choose Eq. (18) and normalize the summed probability to be unit-less by use of the Bohr radius a_0 {15} we obtain:

$$P_{e, \text{norm}} = 4\pi \left(\frac{r + r(\text{vac})}{a_0} \right)^2 R^2. \quad - (19)$$

This expression has assumed that R is hydrogenic, and unaffected by $r(\text{vac})$, so the latter appears only in the pre-multiplying factor. This is an approximation, but in the hydrogen atom an excellent approximation. In other materials it may not be as good an approximation, and Eq. (5) would have to be solved directly with density functional code or another suitable numerical method. Finally the charge density of each orbital is defined to be:

$$\rho = e P_{e, \text{norm}} / V_e \quad - (20)$$

where V_e is an effective volume for each orbital. If a spherical volume is assumed:

$$V_e = \frac{4}{3} \pi r_e^3 \quad - (21)$$

where r is the mean radius of each orbital.
 e

3. SCR AMPLIFICATION MECHANISM.

This mechanism {1-11} is based on a simplified definition of the electric field in ECE theory:

$$\underline{E} = - (\underline{\nabla} + \underline{\omega}) \phi \quad - (22)$$

where $\underline{\omega}$ is the spin connection vector and ϕ is the scalar potential. A simplified form of the Coulomb law of ECE theory is used. This happens to have the same mathematical form as the Coulomb law of Maxwell Heaviside theory:

$$\underline{\nabla} \cdot \underline{E} = \frac{\rho}{\epsilon_0} \quad - (23)$$

The spin connection is assumed to be {1-11}:

$$\omega_r = -\frac{1}{r} \quad - (24)$$

These equations give:

$$\frac{d^2 \phi}{dr^2} + \frac{1}{r} \frac{d\phi}{dr} - \frac{1}{r^2} \phi = -\frac{\rho}{\epsilon_0} \quad - (25)$$

This equation was transformed into an undamped oscillator equation:

$$\frac{d^2 \phi}{dR^2} + \kappa_0^2 \phi = \exp(2i\kappa_0 R) \frac{\rho}{\epsilon_0} \quad - (26)$$

using the Euler transform {16}:

$$\kappa_0 r = \exp(i\kappa_0 R) \quad - (27)$$

Eq. (26) was used to produce a Fourier analysis {1-11} for an assumed cosinal driving term (right hand side of Eq. (26)), and an equivalent circuit was designed. Resonant amplification of ϕ was shown to occur, and this phenomenon was studied in atomic hydrogen {1-11}. It was shown that the SCR mechanism can ionize the hydrogen atom and that the electron thus released could be used to produce electric power. In this section the driving term of Eq. (20) is used in Eq. (25) so that the overall process is shown to be the SCR amplification of the radiative correction.

If the Euler transform method is used, the mathematical problem to be solved is therefore as follows:

$$\frac{d^2 \phi}{dR^2} + \kappa_0^2 \phi = \frac{\rho}{\epsilon_0} \cos(2\kappa_0 R), \quad - (28)$$

$$\rho = \frac{4\pi e}{\epsilon_0 \bar{V}_e} \cdot \left(\frac{\cos^2(\kappa_0 (R + R(\text{vac})))}{a_0^2 \kappa_0^2} \right) R^2(r), \quad - (29)$$

$$r + r(\text{vac}) = \frac{1}{\kappa_0^2} \cos(\kappa_0 (R + R(\text{vac}))), \quad - (30)$$

$$d = \langle d \rangle (1 + \cos(\kappa r)). \quad - (31)$$

However, Eq. (25) can be solved directly by computer and this method is also considered in Section 4.

4. NUMERICAL DEVELOPMENT AND CIRCUIT DESIGNS (by Horst Eckardt)

5. OPTIMUM MATERIALS (by Gareth J. Evans)

4. NUMERICAL DEVELOPMENT AND CIRCUIT DESIGNS

In the following section we discuss results which have been obtained by analytical and numerical studies. First we compare the description of the radiative corrections with the Spin Connection Resonance (SCR) mechanism derived in {17}.

4.1 Parameter studies

From Eqs. (9,11,12) the impact of the fine structure constant α on hydrogenic spectra can be described by the equation

$$-\frac{\hbar^2}{2m} \frac{\alpha}{2\pi} \frac{d^2 P}{dr^2} + (V_{\text{eff}}^{(0)} - V_{\text{eff}}) = 0 \quad (32)$$

with

$$V_{\text{eff}}^{(0)} = -\frac{e^2}{4\pi\epsilon_0 r} + \frac{l(l+1)\hbar^2}{2m r^2} \quad (33)$$

and

$$V_{\text{eff}} = -\frac{e^2}{4\pi\epsilon_0 (r+r(\text{vac}))} + \frac{l(l+1)\hbar^2}{2m (r+r(\text{vac}))^2} \quad (34)$$

If we describe this potential energy difference by a single SCR potential Φ , we have to replace

$$V_{\text{eff}}^{(0)} - V_{\text{eff}} \rightarrow V_{\text{SCR}} \quad (35)$$

and define

$$V_{\text{SCR}} = -e\phi \quad (36)$$

The sign was chosen so that a positive contribution of the potential energy is obtained for high values of Φ . In this way we arrive at the expression

$$e\phi = \frac{e^2}{4\pi\epsilon_0} \left(\frac{1}{r} - \frac{1}{r+r(\text{vac})} \right) - \frac{l(l+1)\hbar^2}{2m} \left(\frac{1}{r^2} - \frac{1}{(r+r(\text{vac}))^2} \right) \quad (37)$$

That this expression makes sense can be seen from considering the limits of vanishing or infinite vacuum interaction, expressed by $r(\text{vac})$:

$$r(\text{vac}) \rightarrow 0 \quad \Rightarrow \quad e\phi \rightarrow 0 \quad (38a)$$

$$r(\text{vac}) \rightarrow \infty \quad \Rightarrow \quad e\phi \rightarrow -V_{\text{eff}}^{(0)} \quad (38b)$$

In the maximum case the SCR potential cancels out the atomic effective potential energy so that Eq. (10) becomes identical to that of a free particle. In general Φ is orbital dependent as was also found in {17} by numerical studies.

In Eq. (37) we have three parameters being of principal interest: Φ , r , and $r(\text{vac})$. In the first three Figures we present the dependence of Φ on $r(\text{vac})$ for fixed r values. Near to the atomic core (Fig. 1, $r=0.1$; all quantities given in atomic units) only the s orbitals ($l=0$) leads to a positive SRC potential, for other orbitals the interaction gives a decrease in potential energy which counteracts a resonance effect. From our earlier studies {18} we know that the vacuum interaction is much smaller than so that a positive SCR effect results. The same holds for a radius in the valence region ($r=1$, Fig. 2). In the outer atomic region ($r=5$, Fig. 3) all contributions become positive, but small. A surface plot $\Phi(r(\text{vac}), r)$ for angular momentum quantum number $l=0$ is presented in Fig. 4. Positive values of Φ are generally obtained for small radii r .

The Figures 5-7 show the dependence of $r(\text{vac})$ from Φ , again for three fixed radii r . There is a pole in $r(\text{vac})$ which moves in direction of $\Phi=0$ for increasing r . Left-hand of the pole we have positive $r(\text{vac})$ values for $l=0$ which show some kind of resonance enhancement when approaching the pole. From the surface plot (Fig. 8) we see that such an enhancement only takes place in a small band of the r - Φ plane.

4.2 Oscillatory $r(\text{vac})$

The results so far were obtained for a non-oscillatory $r(\text{vac})$. Next we use the oscillatory model (3) of the fine structure constant. According to Eq. (12) we have to solve

$$\frac{d^2 P}{dr^2} = \frac{4\pi m}{\hbar^2 \alpha} (V_{\text{eff}}^{(0)} - V_{\text{eff}}) P \quad (39)$$

for the variable $r(\text{vac})$. Using computer algebra {19} this gives a complicated rational function of order 3 in r . In (39) we replace furthermore

$$\alpha = \langle \alpha \rangle (1 + \cos(\kappa r)) \quad (40)$$

with

$$\langle \alpha \rangle = 0.007297 \quad (41)$$

obtaining a solution of (39) which is dependent on a wave number κ . For $P(r)$ we choose the undisturbed radial functions of the Hydrogen atom. Since $P(r)$ depends on the quantum number l , this dependence propagates into the solution of (39). The result for three l values is

graphed in Fig. 9. $r(\text{vac})$ for the 1s orbital strongly oscillates for large radii, but this is in a region where the probability density is very small.

Having obtained the function $r(\text{vac}) (\kappa, r)$, we can proceed now with solving the resonance equation (25). This equation has been transformed into an oscillator equation without damping (26) as was originally described in [17]. The radial coordinate r has been transformed to another coordinate R as given by (27). Therefore we must transform the function $r(\text{vac})(r)$ to $r(\text{vac})(R)$ to be able to use it for the driving charge density $\rho(R)$ at the right-hand side. Unfortunately Eq. (27) is periodic in R and restricted in range. We can construct a bijective mapping for the whole r range by taking the real part of (27) in the form

$$\kappa_0 r = \cos(\kappa_0 R \pm 2\pi n) \quad (42)$$

with an integer n . The inverse transformation then is

$$R = \frac{1}{\kappa_0} (\alpha \cos(\kappa_0 r) \pm 2\pi n) \quad (43)$$

We use this equation to calculate the requested function $r(\text{vac})(R)$. Choosing n in a suitable way, we obtain the behaviour as shown in Fig. 10 where R is continuously defined over the full range of r . The oscillation of α leads to the behaviour shown in Fig. 11 for $r(\text{vac})$ of the 2s orbital. The nonlinear transformation (43) infers the crooked form.

4.3 Resonance

Now we have all elements available to set up Eq. (28) and to construct a numerical solution. By Eqs. (19) and (20) we have

$$\rho(r) = A (r + r(\text{vac}))^2 R_l^2(r) \quad (44)$$

with a normalization factor A which is computed numerically; $R_l(r)$ is the radial wave function of Hydrogen. We transform $\rho(r)$ to $\rho(R)$ by defining a uniform R grid and back-transforming it to an r grid according to (42). Since $\rho(r)$ is given analytically, we can evaluate it on the non-uniform r grid without problems. We can solve now

$$\frac{d^2\phi}{dR^2} + \kappa_0 \phi = f(R) \quad (45)$$

with

$$f(R) = \frac{\rho(R)}{\epsilon_0} \cos(2\kappa_0 R) \quad (46)$$

In order to obtain resonances in the solution, we had to make two modifications: The relative strength of $r(\text{vac})$ in Eq. (44) had to be enhanced by a factor of 1000 and the driving force (46) had to be enhanced by the same factor as well. While the latter is an uncritical operation due to the unspecified normalization factor in (44), the enhancement of $r(\text{vac})$ can be made plausible by the following: This calculation is restricted to a single atom where $\rho(R)$ is constrained to a few Bohr radii. In an atomic lattice of a solid, the excitation goes over many atoms where resonance can enhance this in a nearly unbound spatial region. Therefore it

may be justified to enlarge $r(\text{vac})$ in this model calculation. As an additional approximation we identify the two wave numbers κ and κ_0 in Eqs. (40) and (46) as we did in earlier SCR calculations {17}.

The driving charge density thus enhanced is graphed in Fig. 12. The two maxima of the atomic 2s distribution are still visible, strongly superimposed with oscillations. The total driving force is shown in Fig. 13. The zero at $R=3$ is propagated from the zero in Fig. 12. Finally we present the numerical solution $\Phi(R)$ in Fig. 14. One can see that there is a resonance for the second wave number $\kappa=5$. Since $f(R)$ is restricted in space, the resonance does not grow further outside the “definition volume”. This behaviour reflects the above discussion about the restrictions of the model.

The resonance behaviour is clearly seen from the resonance diagram, Fig. 15. The maximum of the amplitude taken over 15 wave lengths is plotted. The main peak is at half the frequency of a pure cosine driving force $\cos(\kappa_0 r)$, and there are several secondary maxima visible. The structure is somewhat richer than for the earlier SCR calculation {17}, but has the feature of the halved resonance frequency in common with it.

4.4 Relation to Circuits and SCR applications

The resonance equation (45/46) can technically be realized by an equivalent circuit as already described in detail in {17}. The driving force has to be provided electrically. This force is characterized by its Fourier spectrum. However, we do not have a continuously periodic function as in {17} since one single atom which is considered in our model is not a periodic structure. Therefore we choose the usual proceeding in such cases: we cut the function $f(R)$ at an appropriate radius (here $R=15$) and assume periodicity with a wavelength of $\lambda=15$. For each given κ we obtain separate functions $f(R, \kappa)$, i.e. different Fourier spectra for each κ value. These are shown in Fig. 16 for the three κ values investigated. The structures are similar but shifted in frequency. This means that there is a common pattern in the structure of the driving force. This could be like a “fingerprint” for a certain atomic structure.

Another type of SCR devices are the various types of Bedini motors, or more precisely, motor-generators {20}. According to the block diagram of Fig. 17, they consist of a motor part, a generator part, and a control circuit. The generator part which takes up the potential from spacetime is a series resonance circuit as can be seen from the diagram. The motor and the control part are there to generate a suitable form of the driving force and are coupled inductively. We must restrict comparison to this logical level. It should become clear that the functioning of the Bedini motor-generator is based on the principle that we have derived from the equivalent circuit. A more direct application of the mechanisms can take place in solid state chemistry as is discussed in the next section.

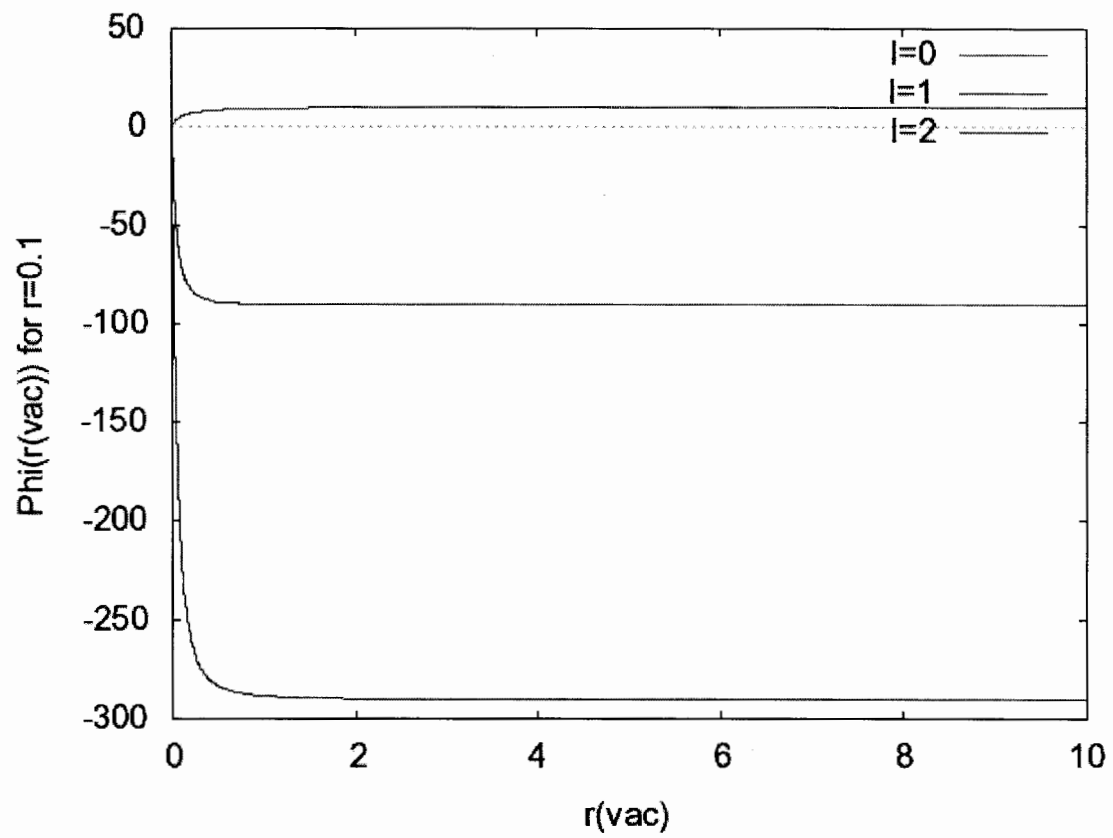


Fig. 1. $\Phi(r(\text{vac}))$ for fixed $r=0.1$.

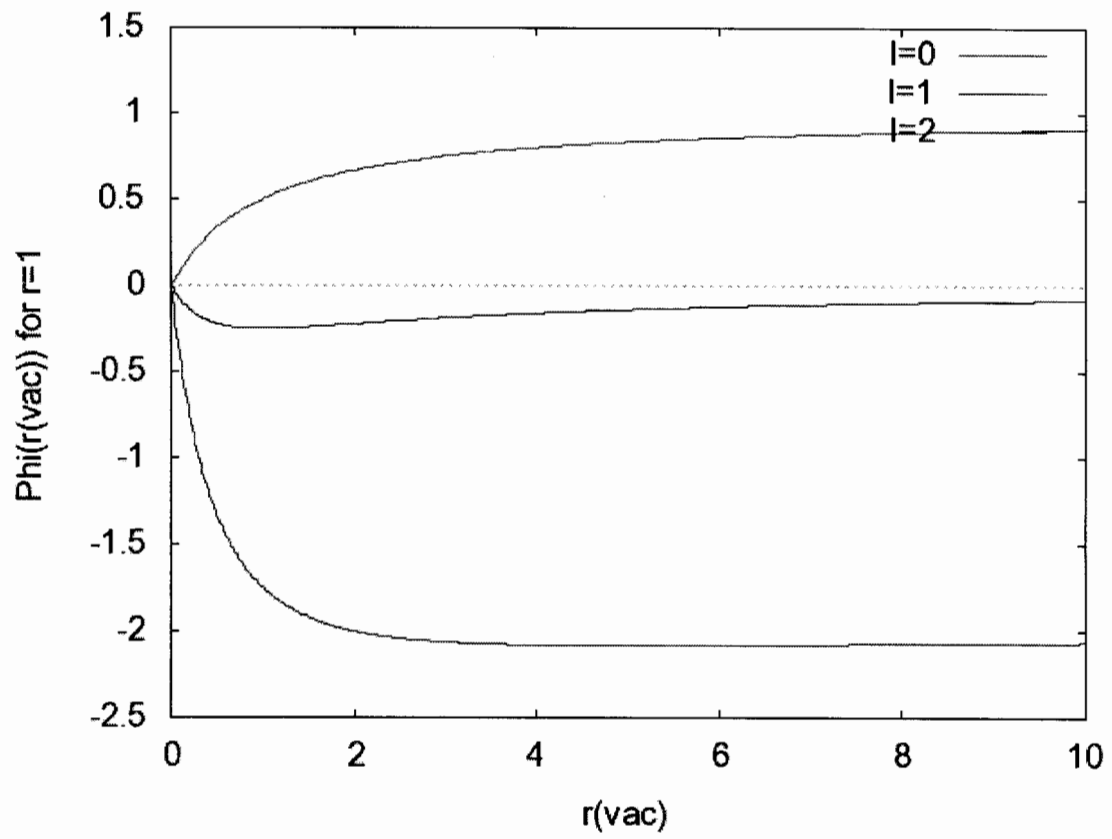


Fig. 2. $\Phi(r(\text{vac}))$ for fixed $r=1$.

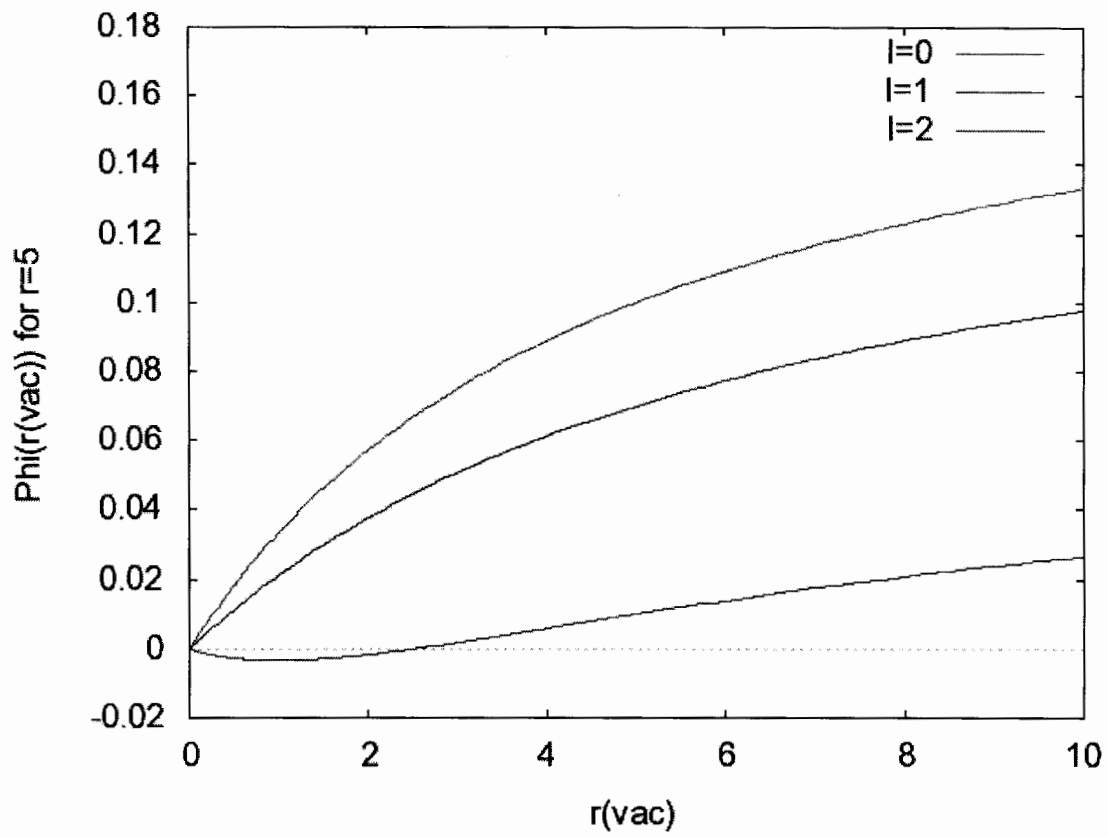


Fig. 3. $\Phi(r(\text{vac}))$ for fixed $r=5$.

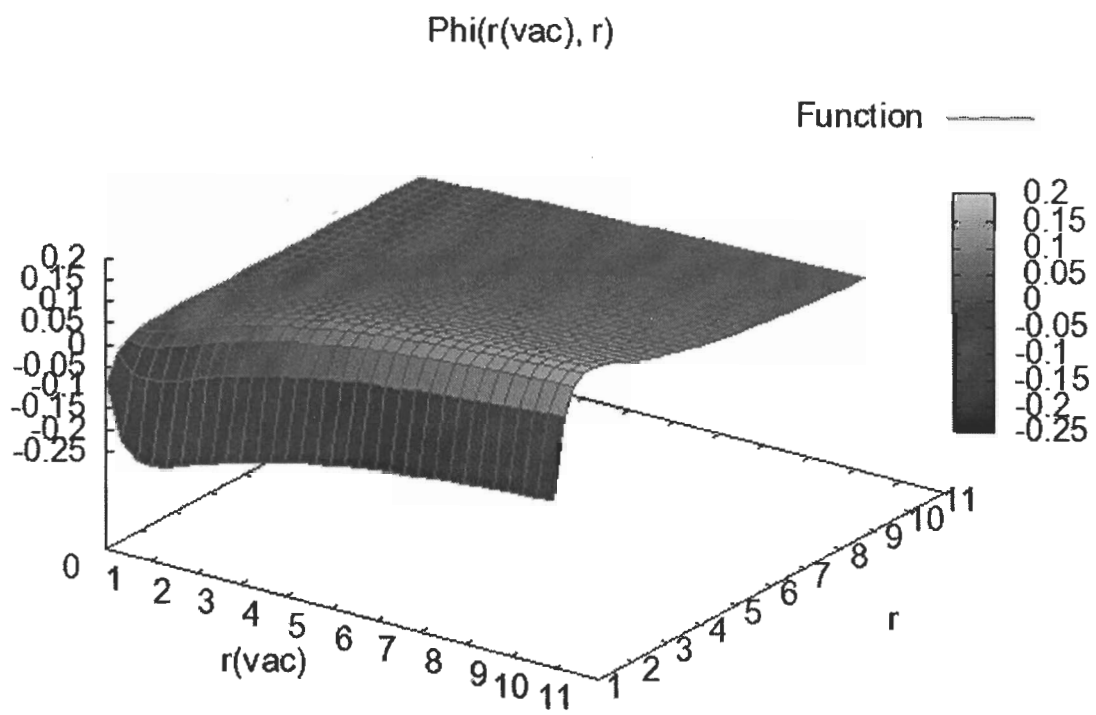


Fig. 4. Surface plot $\Phi(r(\text{vac}), r)$ for angular momentum quantum number $l=0$.

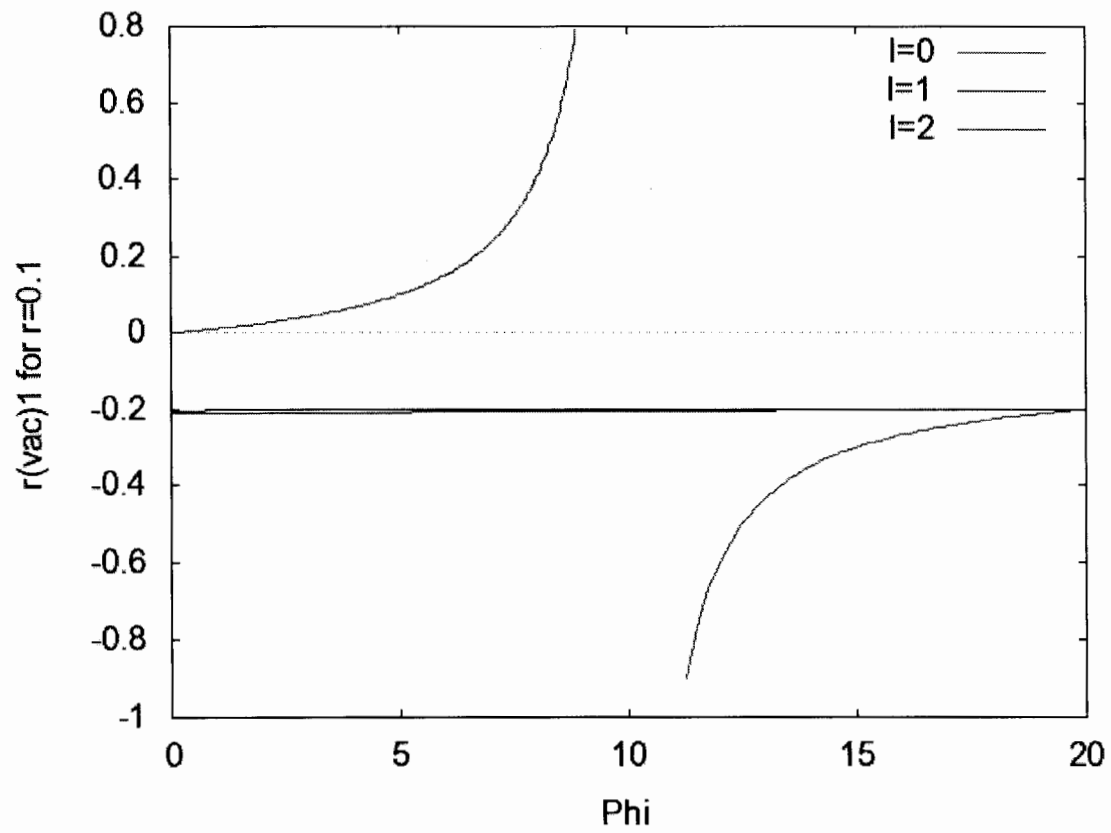


Fig. 5. $r(\text{vac})_1(\Phi)$ for fixed $r=0.1$.

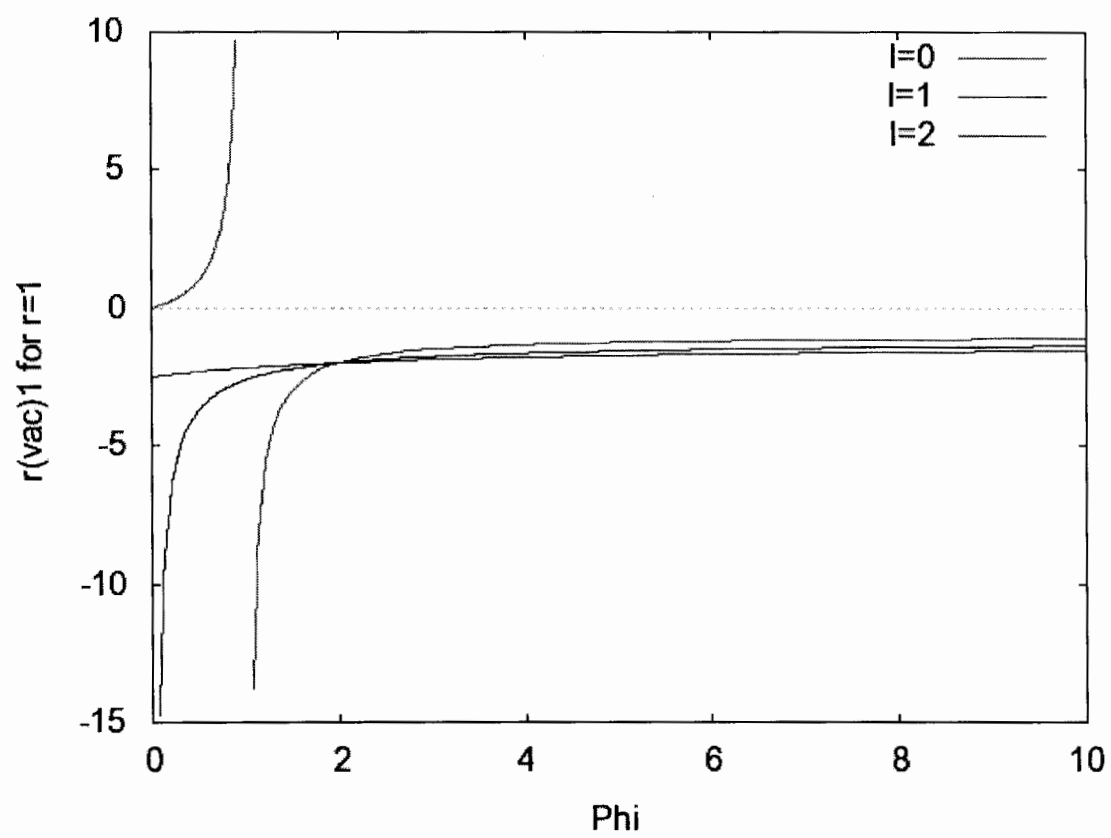


Fig. 6. $r(\text{vac}) (\Phi)$ for fixed $r=1$.

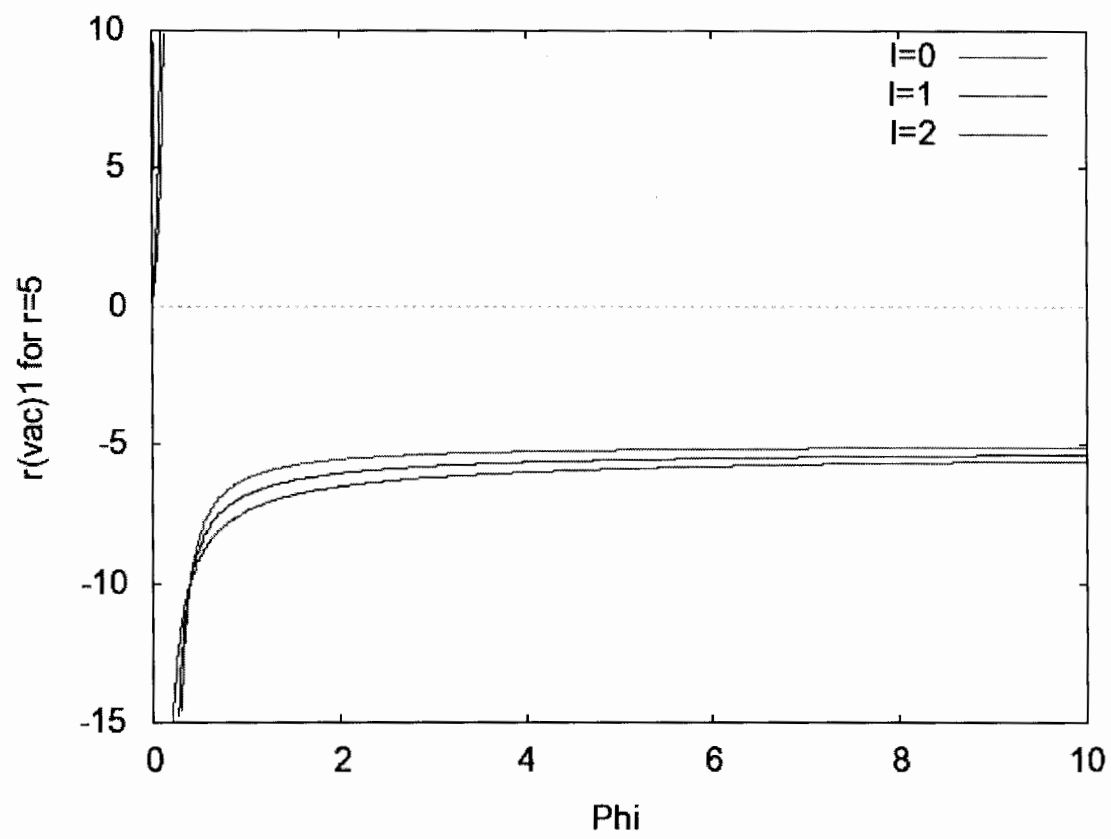


Fig. 7. $r(\text{vac}) (\Phi)$ for fixed $r=5$.

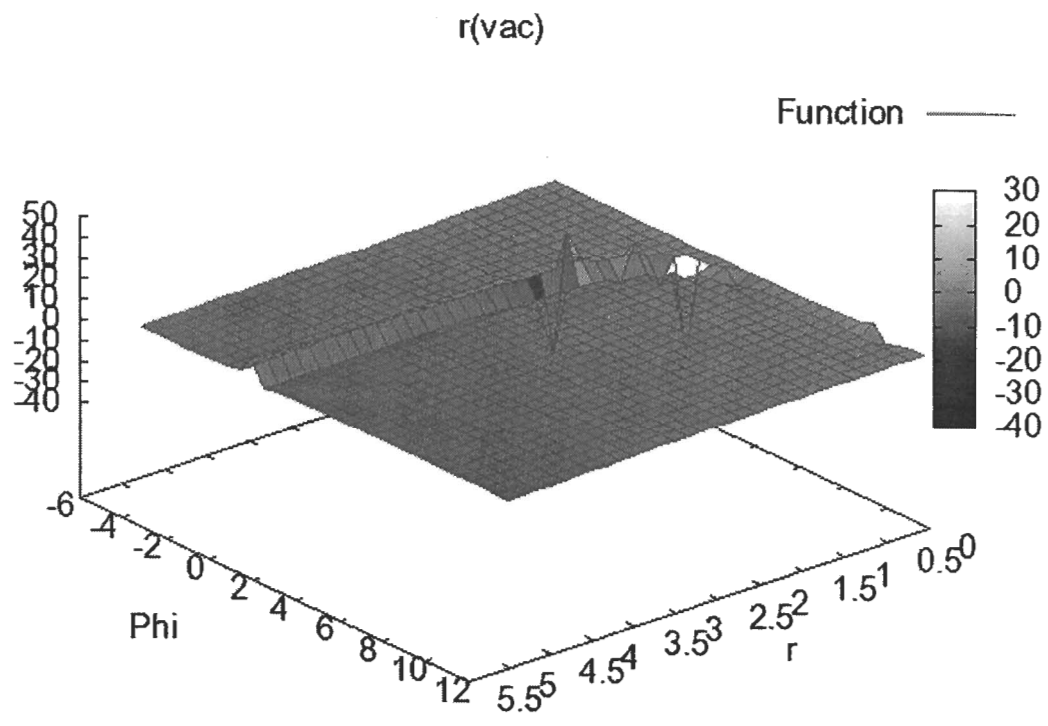


Fig. 8. Surface plot $r(\text{vac}) (\Phi, r)$ for angular momentum quantum number $l=0$.

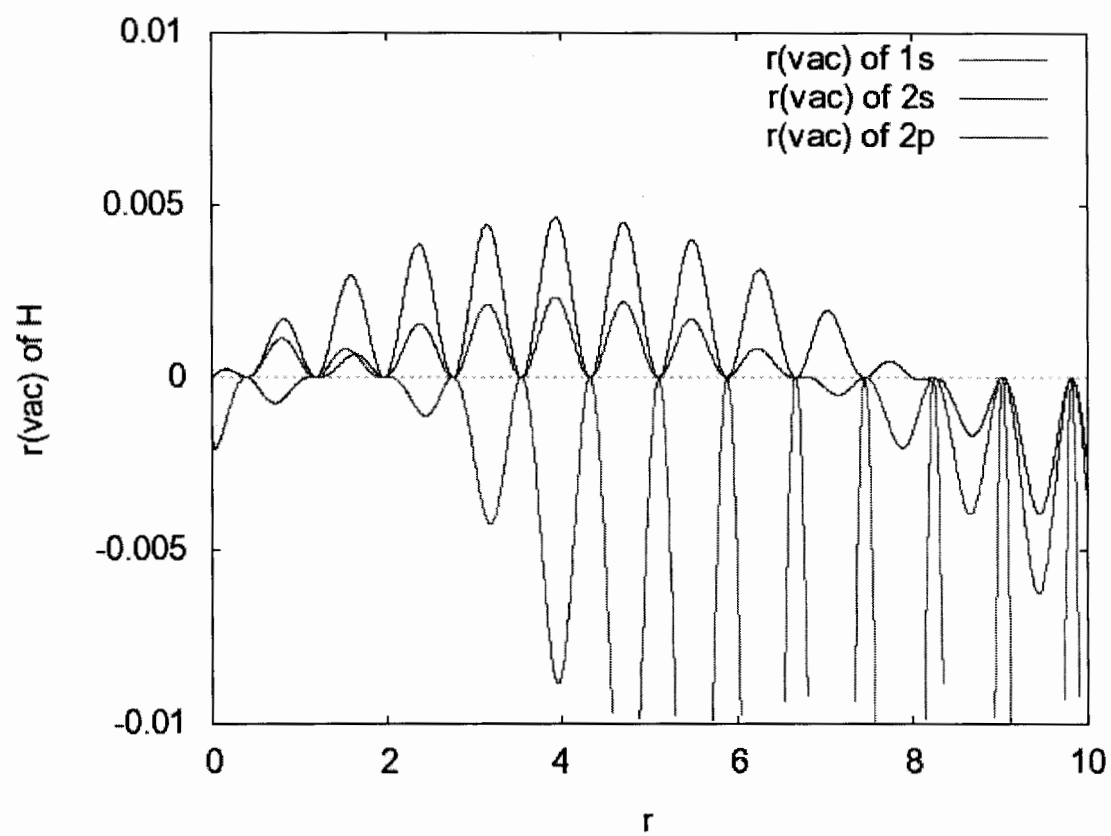


Fig. 9. Oscillating $r(\text{vac})$ for three orbitals of H for $\kappa=8$.

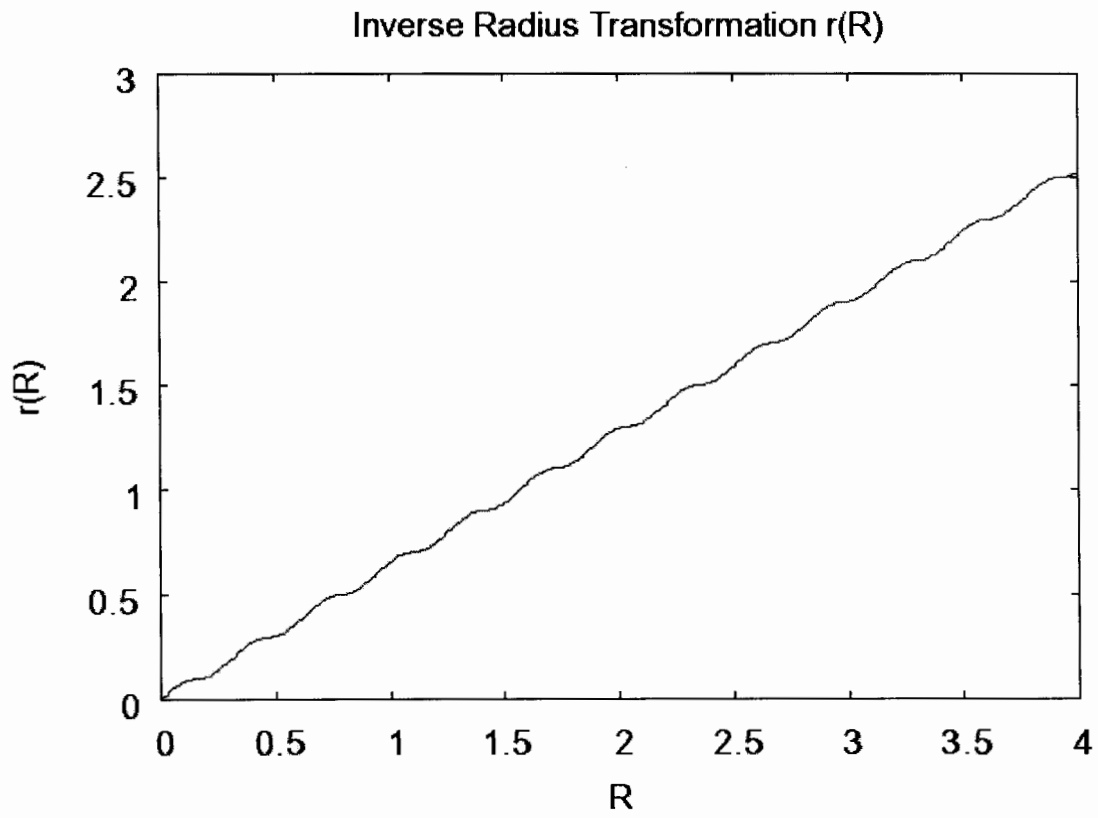


Fig. 10. Radius back transformation $r(R)$.

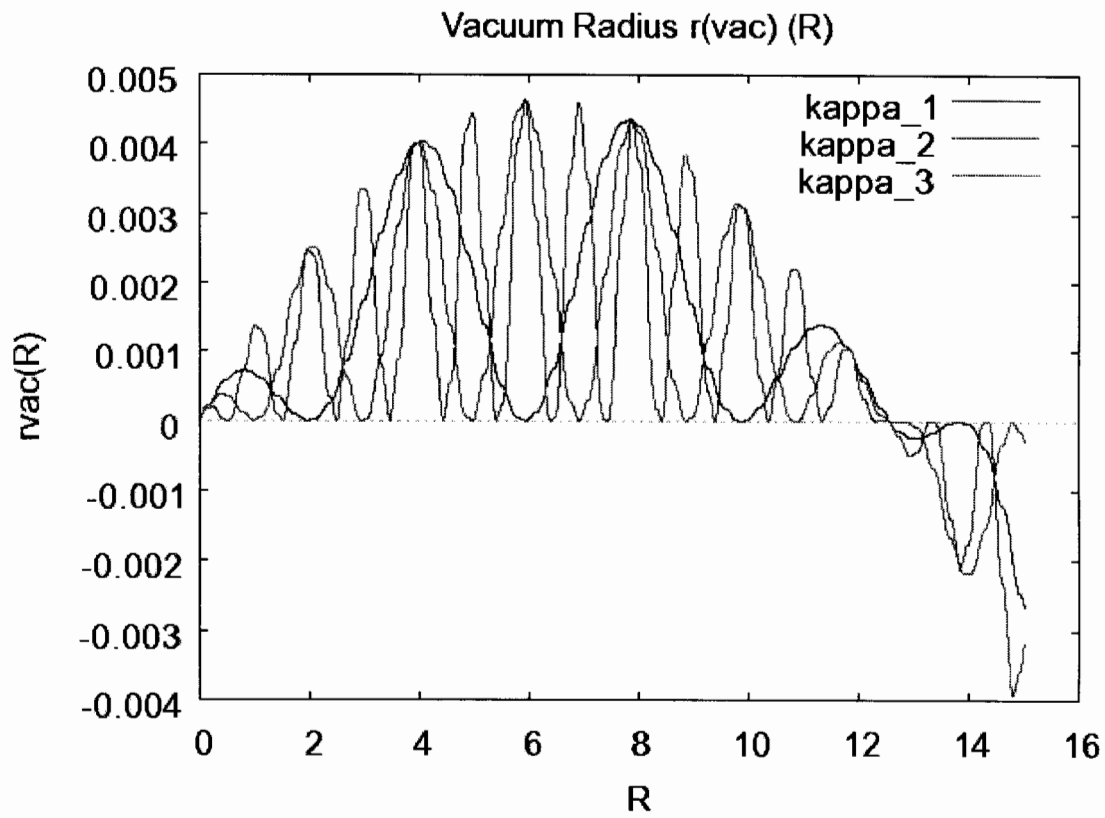


Fig. 11. Oscillating vacuum radius $r(\text{vac})$ (R) of the 2s orbital for three wave numbers (2.5, 5, 10).

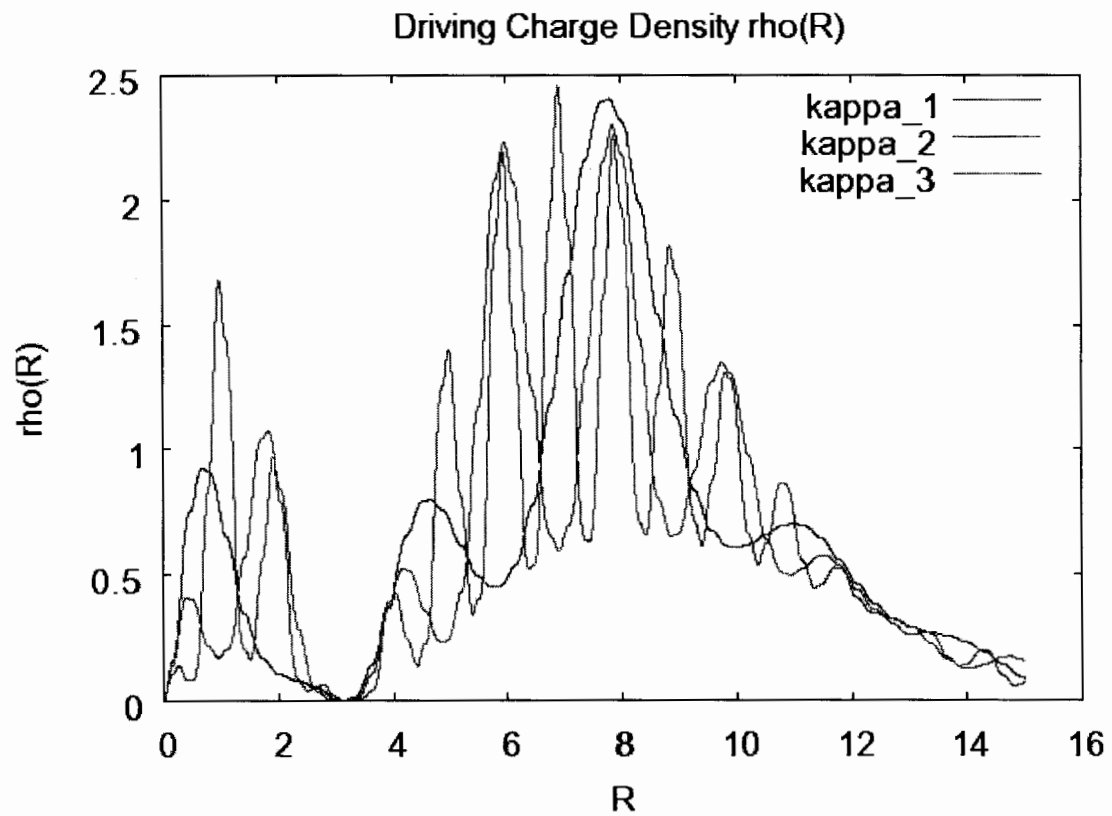


Fig. 12. charge density of driving charge density $\rho(R)$ equation for three wave numbers (2.5, 5, 10).

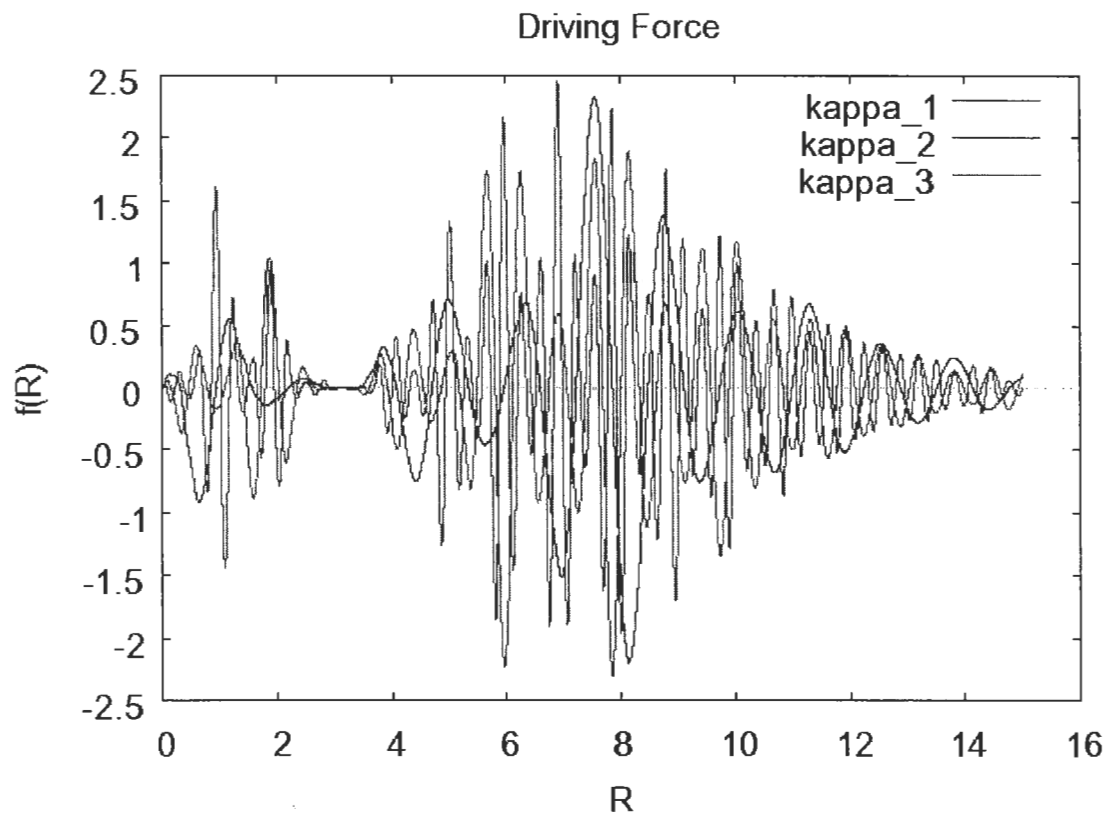


Fig. 13. Driving force $f(R)$ for for three wave numbers (2.5, 5, 10).

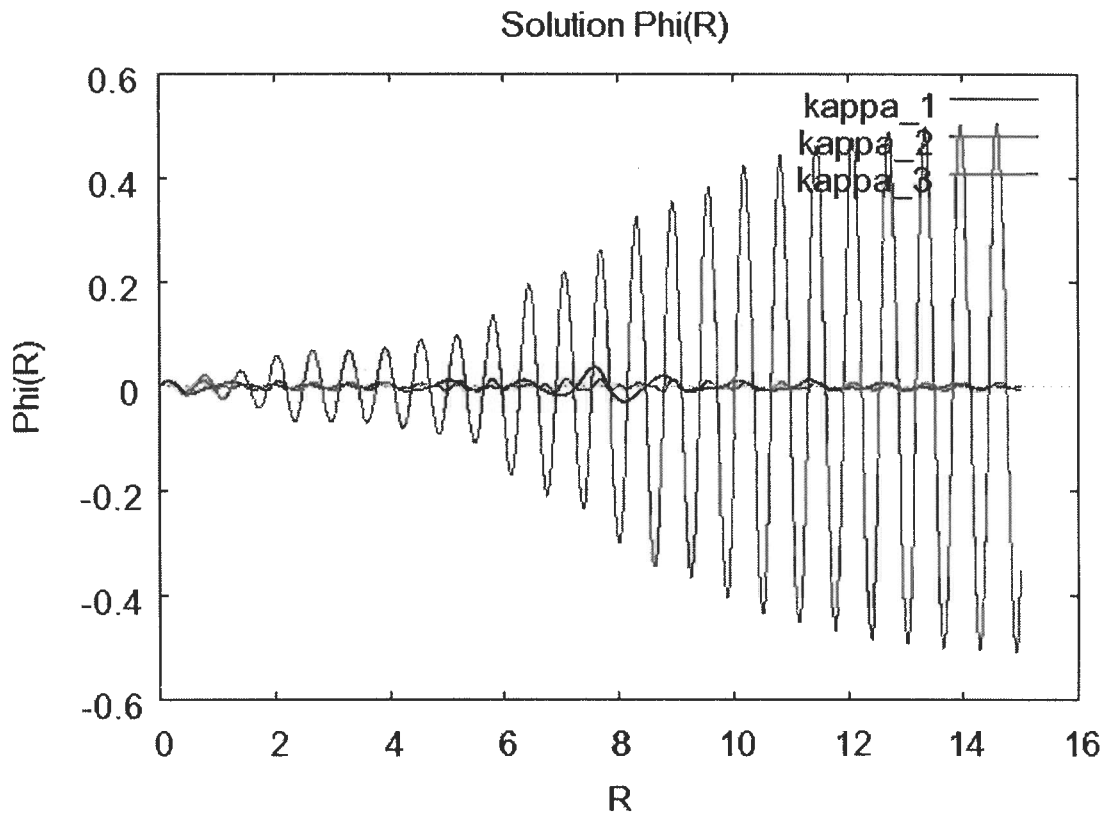


Fig. 14. Solution of $\Phi(R)$ of Euler transformed equation for three wave numbers for three wave numbers (2.5, 5, 10).

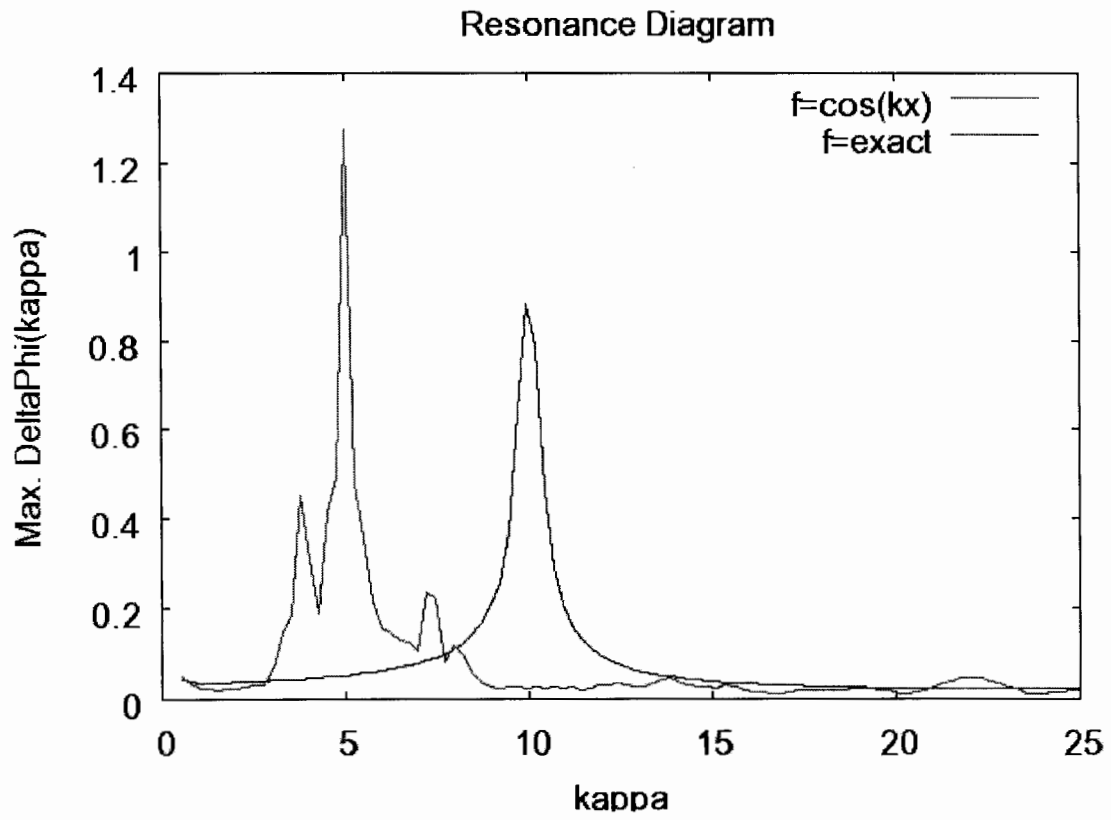


Fig. 15. Resonance diagram, max. amplitude after 15 wavelengths $\lambda=2\pi/\kappa$.

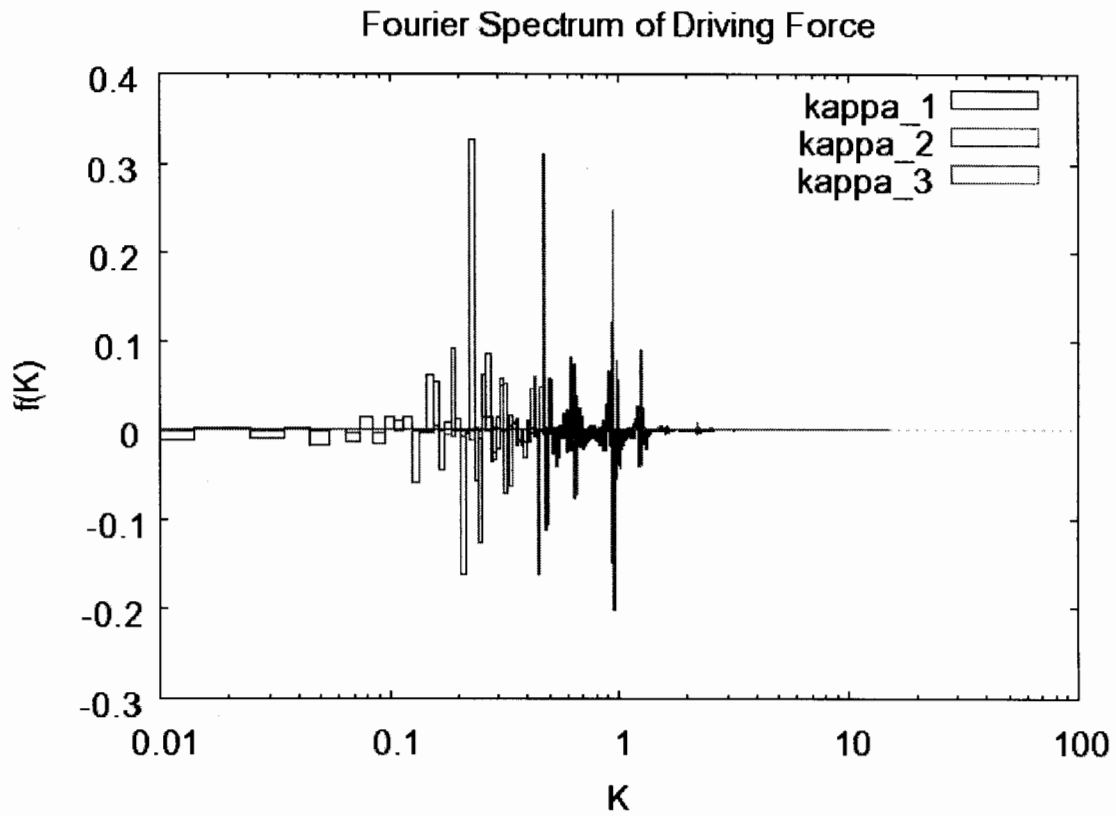


Fig. 16. Fourier transform of driving force for three wave numbers (2.5, 5, 10).

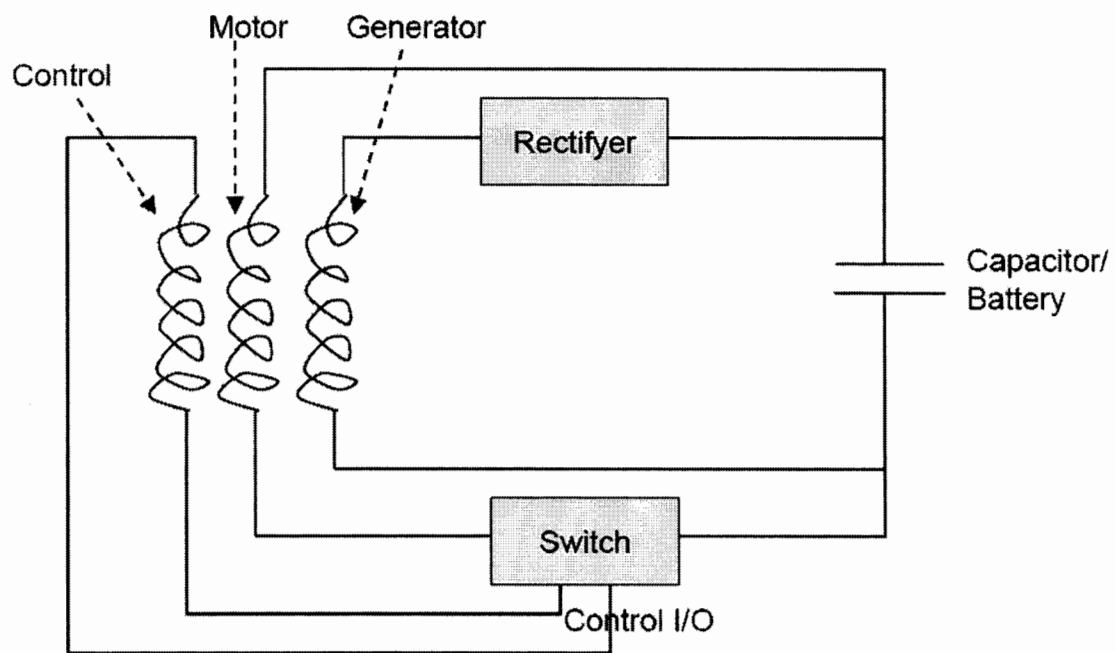


Fig. 17. Block diagram of Bedini motor-generator.

ACKNOWLEDGMENTS

The British Government is thanked for a Civil List Pension to MWE for distinguished contributions to science, and the staff of AIAS and many others are thanked for invaluable voluntary work and many interesting discussions.

REFERENCES

- {1} M. W. Evans, "Generally Covariant Unified Field Theory" (Abramis Academic, Suffolk, 2005), vol. 1.
- {2} M. W. Evans, *ibid.*, Volumes 2 and 3 (2006).
- {3} M. W. Evans, *ibid.*, vols. 4 and 5 in prep. (Papers 55 to 87 on www.aias.us).
- {4} L. Felker, "The Evans Equations of Unified Field Theory" (Abramis Academic, Suffolk, 2007, in press); A. D. DeBruhl, "The Ultimate Truth" (Published Oct 2006, amazon).
- {5} H. Eckardt, L. Felker, D. Indranu, S. Crothers, K. Pendergast and G. J. Evans, contributions on www.aias.us.
- {6} M. W. Evans, precursor gauge theories to ECE, Omnia Opera Section of www.aias.us, 1992 to present.
- {7} M. W. Evans and L. B. Crowell, "Classical and Quantum Electrodynamics and the B(3) Field" (World Scientific, 2001).
- {8} M. W. Evans, ed., "Non-Linear Optics", a special topical issue in three parts of I Prigogine and S. A. Rice (series editors), "Advances in Chemical Physics" (Wiley, New York, 2001, second edition hardback and e book), vols. 119(1) to 119(3), endorsed by the Royal Swedish Academy; *ibid.*, M. W. Evans and S. Kielich (eds.), first edition, (Wiley, New York, 1992, 1993 and 1997 (softback)), vols. 85(1) to 85(3), prize for excellence, Polish Government.
- {9} M. W. Evans and J.-P. Vigi er, "The Enigmatic Photon" (Kluwer, Dordrecht, 1994 to

2002, hardback and softback) in five volumes.

{10} M. W. Evans and A. A. Hasanein, "The Photomagnetron in Quantum Field Theory"

(World Scientific, 1994).

{11} M. W. Evans, Acta Physica Polonica, ^B38, 2211 (2007).

{12} S. P. Carroll, "Space-time and Geometry: an Introduction to General Relativity"

(Addison Wesley, New York, 2004, also available on web), chapter three. See also the papers by D. Indranu on www.aias.us on advanced Cartan geometry.

{13} S. Weinberg, "The Quantum Theory of Fields" (Cambridge Univ. Press, 2005, softback).

{14} L. H Ryder, "Quantum Field Theory" (Cambridge Univ. Press, 1996, softback).

{15} P. W. Atkins, "Molecular Quantum Mechanics" (Oxford Univ. Press, 1983, 2nd. Ed., and many subsequent editions in softback).

{16} G. Stephenson, "Mathematical Methods for Science Students" (Longmans, London, 1968, fifth impression softback and subsequent impressions).